Development of a Strapdown Gyrocompass on Base of Fiber-Optic Gyroscope

P. K. Plotnikov, A. V. Mikheyev, Yu.V. Chebotarevsky

Saratov State Technical University
Polytechnicheskaya str. 77
410054 Saratov
RUSSIA

Yu. N. Korkishko, V. A. Fedorov,
V. E. Prilutskii, V. G. Ponomarev

Optolink, Ltd.,
Zelenograd
„Proton" Facility
103948 Moscow
RUSSIA

Symposium Gyro Technology 2004
Stuttgart, Germany

Problem statement. Recent developments of fiber optical gyroscopes (FOG) and accelerometers in the USA, France, Germany and Russia have led to the creation of instruments characterized by the values of drift and instabilities of zero bias of $5 \cdot 10^{-3},....10^{-2}$ deg/hour and $5 \cdot 10^{-5} g$. Such parameters are sufficient for making strapdown gyrocompass on the base of FOGs and precise quartz accelerometers. These units mounted in a housing and arranged with onboard computer are actually the strapdown inertial navigation system (SINS). Nowadays many companies in the world produce similar three-axis systems (for instance strapdown gyrocompass Octans (France), KVH Industries (USA), SFIM Industries (Deutschland, GmbH) [1-4], gyrohorizoncompass (CSRI "Electropribor" [5], Russia) etc). In particular, these systems are widely used on hydrographic and other ships. Some results of development of the original strapdown gyrocompass are presented in this work. The structure of the developed instrument is same as mentioned systems. Theoretical analysis has shown that application of precise FOGs and accelerometers gives the possibility to obtain the technical parameters and price of SGC unit comparable with above mentioned systems. The considered system is based on FOGs and accelerometers developed and produced by Russian company "Optolink Ltd". Note that SGC based on horizon-scanning FOGs are not considered in this paper [6,7].

Problem solution. The combination of a principle of computer modeling of place vertical under the Schuler's conditions of undisturbance to the action of horizontal absolute accelerations [4,8-10] and the condition of coincidence of one of horizontal axes of a trihedron with a north direction makes it possible to realize the gyrocompass model. It is necessary to note that the system is intended for application on mobile objects (MO) with the limited pitch angles $|\theta| < 75,...,80^0$. Therefore Euler's kinematic equations for Euler-Krylov's angles are used as the algorithms basis. Also the kinematic quaternion algorithms are compared with developed model. In this approach (see Ref. [11,12]) the angular rates are related to horizontal and the Euler-Krylov's angles are applied.

The trigonometrical algorithms of an initial alignment which provide the autonomy, concerning the use of signals of only inertial sensors present the special group of orientation and navigation algorithms.

The basis of given strapdown gyrocompass (SGC) are the inertial navigating system (SINS) made on the basis of the unit of three optical fibre gyroscopes (FOG), forming triade of mutually orthogonal measuring devices of angular rate (TMDAR) , and on the basis of the unit of three measuring devices of specific force of object (MSF), forming triade of mutually orthogonal measuring devices of specific force (TMSF), and onboard computer (OC) with the interface (fig. 1).

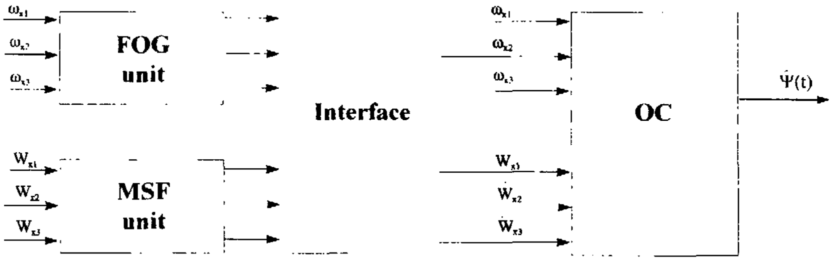

Fig. 1

In fig. 1 $\omega_{xi}, W_{xi} (i=\overline{1,3})$ are the components of absolute angular rate and specific forces of object; $\hat{\omega}_{xi}, \hat{W}_{xi} (i=\overline{1,3})$ are the estimations of the mentioned above components that are entered in OC; $\hat{\Psi}(t)$ is the estimation of a course angle at output of OC. In order to explain the process of functioning SGC the scheme of orthogonal geographical accompanying reference frame (RF) $o\zeta_i (i=\overline{1,3})$ is shown in fig. 2. Also there are shown free in an azimuth horizon accompanying RF, $o\eta_i (i=\overline{1,3})$ RF $ox_i (i=\overline{1,3})$, bound with object (ox_1 - lenghtwise, ox_2 - normal axes) and turns of reference frame ox_i on course angle Ψ, pitch angle θ and a roll angle γ; ψ is azimuth angle. In fig. 3 mutual position of unrotatable ($\bar{\omega}_{\eta 2}=0$) in an azimuth horizon accompanying RF $o\eta_i (i=\overline{1,3})$ and reference frame $o\zeta_i (i=\overline{1,3})$ is represented. Their vertical axes $o\eta_2$ *and* $o\zeta_2$ are coincided, the angle ϑ defines a turn of RF $o\eta_i$ that is relative to RF $o\zeta_i$ on an azimuth in a plane of horizon. It is the angle introduced in [13, pp. 450-474]. In fig. 3 ox'_1, ox'_3 are axes of RF $ox_i (i=\overline{1,3})$, projected on a horizontal plane. Accounting the ellipsoidality of the Earth, we have the following kinematic equations [14]:

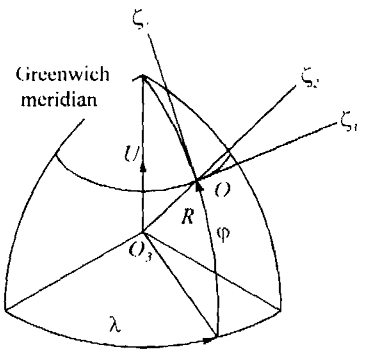

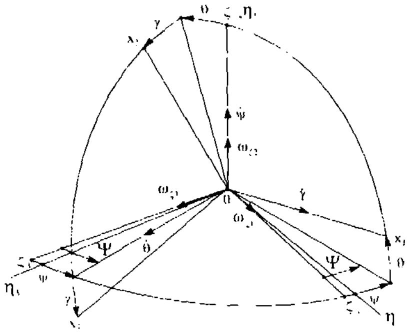

Fig.2

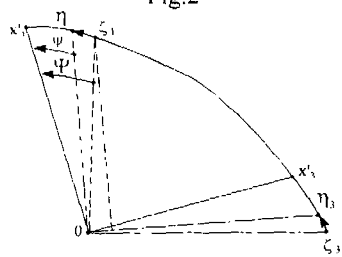

Fig.3

$$
\left.
\begin{aligned}
&\overline{\omega}_{\zeta1} = \frac{V_{\zeta3}}{R_1} = \dot{\Lambda}_a \cos\varphi; \quad R_1 = \frac{R}{\chi}; \qquad R = a + h; \\
&\overline{\omega}_{\zeta2} = \frac{V_{\zeta3}}{R_1} tg\varphi = \dot{\Lambda}_a \sin\varphi; \qquad V_{\zeta3} = R_1 U \cos\varphi + v_{\zeta3}; \\
&\overline{\omega}_{\zeta3} = -\dot{\varphi} = -\frac{V_{\zeta1}}{R_2}; \qquad V_{\zeta1} = v_{\zeta1}; \qquad R_2 = \frac{(a+h)(1-e^2)}{\chi^3}; \\
&\chi = \sqrt{1 - e^2 \sin^2\varphi}; \qquad e^2 = \frac{(a^2 - b^2)}{a^2}; \qquad \dot{h} = \frac{v_{\zeta2}}{\chi}; \;\; V_{\zeta2} = v_{\zeta2},
\end{aligned}
\right\}(a)
\qquad (1)
$$

$$
\left.
\begin{aligned}
&\overline{\omega}_{\eta1} = \overline{\omega}_{\zeta1} \cos\vartheta - \overline{\omega}_{\zeta3} \sin\vartheta \\
&\overline{\omega}_{\eta3} = \overline{\omega}_{\zeta3} \cos\vartheta + \overline{\omega}_{\zeta1} \sin\vartheta \\
&\overline{\omega}_{\eta2} = \overline{\omega}_{\zeta2} + \dot{\vartheta} = 0; \;\; \dot{\vartheta} = -\overline{\omega}_{\zeta2}
\end{aligned}
\right\}(b)
$$

there $v_{\zeta i}, V_{\zeta i} (i = \overline{1,3})$ are components of relative and absolute velocities of some point O of housing of SGC by the axes of an accompanying trihedron $O\zeta_i (i = 1,2,3)$ which axis $O\zeta_2$ coincides with a vector of acceleration of a gravity, the axis $O\zeta_1$ is directed to the North; h is height of a point O, measured from point O_y, for which $h = h_0$. With $h < 0$ we have depth of dipping of SGC; φ is geographical latitude; Λ_a, λ are an absolute and geographical longitude; a, b are larger and smaller axes of ellipsoid; U is the angular rate of the Earth; e^2 is a square of the first eccentricity. We shall note, that formulas (1) are right for spherical model of the Earth when $e=0$. For initial point O_v at the beginning of movement the coordinate of a site it is designated as follows:

$$h_0;\ \lambda_0;\ \varphi_0;\ \Lambda_0 = U(t - t_0) + \lambda_0 \qquad (2)$$

also we accept them for coordinates of undisturbed movement, λ_0, φ_0 are an initial geographical longitude and latitude; t_0 is the initial moment of time. With the taking into account (2) coordinates of the disturbed movement we shall present in the following kind:

$$h = h_0 + H; \qquad \Lambda_a = \Lambda_0 + \Lambda; \qquad \varphi = \varphi_0 + \Phi, \quad \lambda = \lambda_0 + \Lambda. \qquad (3)$$

there $H;\Lambda;\Phi$ are increments of coordinates in relation to coordinates of initial point O_v. $\bar{\omega}_{\zeta_i}(i=\overline{1,3})$ are components of absolute angular rates of RF $o\zeta_i(i=\overline{1,3})$; $\overline{\omega}_{\eta_i}(i=\overline{1,3})$ are absolute angular rates of RF $o\eta_i(i=\overline{1,3})$; $\omega_{\zeta_i}, \omega_{\eta_i}(i=\overline{1,3})$ are the projections of absolute angular rates of MO on axes of RF $o\zeta_i$ and $o\eta_i$ accordingly.

Relations (1) - (7) are intended for use in algorithms of functioning SGC with account of the nonspericality of the Earth, and also for mathematical modeling of functioning of SGC. A is a matrix of directing cosines, determined from transformation $[x_1 x_2 x_3]^T = A[\eta_1 \eta_2 \eta_3]^T$ by the following expression:

$$A_1 = \begin{bmatrix} \cos\psi\cos\theta & \sin\theta & -\sin\psi\cos\theta \\ -\cos\psi\sin\theta\cos\gamma + \sin\psi\sin\gamma & \cos\theta\cos\gamma & \sin\psi\sin\theta\cos\gamma + \cos\psi\sin\gamma \\ \sin\psi\cos\gamma + \cos\psi\sin\theta\sin\gamma & -\cos\theta\sin\gamma & \cos\psi\cos\gamma - \sin\psi\sin\theta\sin\gamma \end{bmatrix} \qquad (4)$$

For transformation RF we have: $[x_1 x_2 x_3]^T = A^{\vartheta} A[\zeta_1 \zeta_2 \zeta_3]^T$ (5)

$$A^{\Psi} = A^{\vartheta} A; \; A^{\vartheta} = \begin{bmatrix} \cos\vartheta & 0 & -\sin\vartheta \\ 0 & 1 & 0 \\ \sin\vartheta & 0 & \cos\vartheta \end{bmatrix} \qquad (6)$$

After multiplication $A^{\vartheta}A$ the matrix A^{Ψ} with account of $\Psi = \psi + \vartheta$ will look like a matrix A with replacement of angle ψ by angle Ψ. Absolute angular rates of reference frame $ox_i(i=\overline{1,3})$ bound to mobile object (MO), look like:

$$\omega_{x1} = \bar{\omega}_{x1} + \dot{\gamma} + \dot{\psi}\sin\theta; \qquad \begin{bmatrix} \omega_{x1} \\ \bar{\omega}_{x2} \\ \bar{\omega}_{x3} \end{bmatrix} = A \begin{bmatrix} \omega_{\eta 1} \\ 0 \\ \bar{\omega}_{\eta 3} \end{bmatrix} = A^{\Psi} \begin{bmatrix} \bar{\omega}_{\zeta 1} \\ \bar{\omega}_{\zeta 2} \\ \bar{\omega}_{\zeta 3} \end{bmatrix}$$
$$\omega_{x2} = \omega_{x2} + \dot{\psi}\cos\theta\cos\gamma + \dot{\theta}\sin\gamma;$$
$$\omega_{x3} = \bar{\omega}_{x3} + \dot{\theta}\cos\psi - \dot{\psi}\cos\theta\sin\gamma; \tag{7}$$

For signals (estimations) of TMDAR and TMSF next formulas are used:

$$[W_{x1} W_{x2} W_{x3}]^T = A^{\Psi}[W_{\zeta 1} W_{\zeta 2} W_{\zeta 3}]^T; \; [\omega_{x1} \omega_{x2} \omega_{x3}]^T = A^{\Psi}[\omega_{\zeta 1} \omega_{\zeta 2} \omega_{\zeta 3}]^T;$$
$$\hat{\omega}_{xi} = \omega_{xi} + \Delta\omega_{xi}, \; \hat{W}_{xi} = W_{xi} + \Delta W_{xi} \; \left(i = \overline{1,3}\right), \tag{8}$$

there $\Delta\omega_{xi}, \Delta W_{xi}$ - FOGs drifts and zero biases of MSF. So, algorithms of functioning of SGC are constructed on the basis of Euler's kinematic equations with the including terms of correction just as it is described in [11], with leading of angular rates by signals of FOGs, specific forces by signals of TMSF and angular rates of correction to horizon basis just as it is described in [12]. Thus Euler - Krylov's angles are used. From (1) - (3) we can see, that due to the Earth nonspericality algorithms become complicated, and Schuler's conditions in north and east directions are different [15].

Types and parameters of horizontal and azimuthal correction, their switching on various modes of movement of mobile object (MO) are determined. The possibility of application of gyroazimuth in SGC modes for high latitudes, and in other cases (at geographical latitude up to 75-80^0 – of gyrocompass mode) is investigated. With mathematical modeling the system was considered on the basis of application FOGs of model PNSK 40-002 produced by company "Optolink", having drift 0,02 deg/hours and the range of measurements 30 deg/sec, accelerometers such as AK-6 and KCA-100. Mathematical modelling of functioning SGC mounted on MO which making angular and linear motions has shown that:

- Error of the course angle with using FOGS such as PNSK 40-002 and accelerometers such as AK-6 has made 9 arc minutes after 5,5 hours of continuous work (in PNSK 40-002 scale factor deviation is 0,1 %; in AK-6 zero bias is 10^{-4} m/s^2, a scale factor deviation is 0,01 %). Thus Schuler's frequency in a direction North - South is higher, than in a direction the East - West at $\varphi \cong 45^0$ by 0,17 %. Not spherical model of the Earth and a equations (1) - (8) are used.

- Modeled a variant of application of accelerometers such as Analog Device instead of precision and expensive AK-6. The spherical model of the Earth is used. Thus in (1) - (3) we put $h=0$, $R=6371$ *km* - radius of the spherical Earth; it is followed from these formulas that value of h influence to the Schuler's conditions.

Time of initial alignment of GC FOG is about 200 seconds that is comparable with time of alignment of French gyrocompass Octans.

Experimental researches are done. In experiments the unit of three FOG PNSK 40-003, similar PNSK 40-002, and three micromechanical accelerometers ADXL05AH (this unit is named SIIM), mounted on one arm has been used. The interfaces connected to ports RS485 of personal computer Pentium-4 are used as devices of communication. The photography of unit SIIM mounted on rotary platform CRA-5, is shown in fig. 4. SIIM is fixed on a platform of the rotary platform CRA-5 providing unlimited turns on a angle of a course, on the limited angles of pitch θ and roll γ (up to $\pm 40^0$ at accuracy of the setting of angles $0,1^0$). The basis is horizonted on a level with accuracy ±1'. System SGC was functioning in real time. Constant components of drifts of FOGs and zero biases of accelerometers are about 0,5, ..., 1, deg/hour and 0.2, ..., 0,5, m/s^2 . They have been determined and algorithmically compensated.

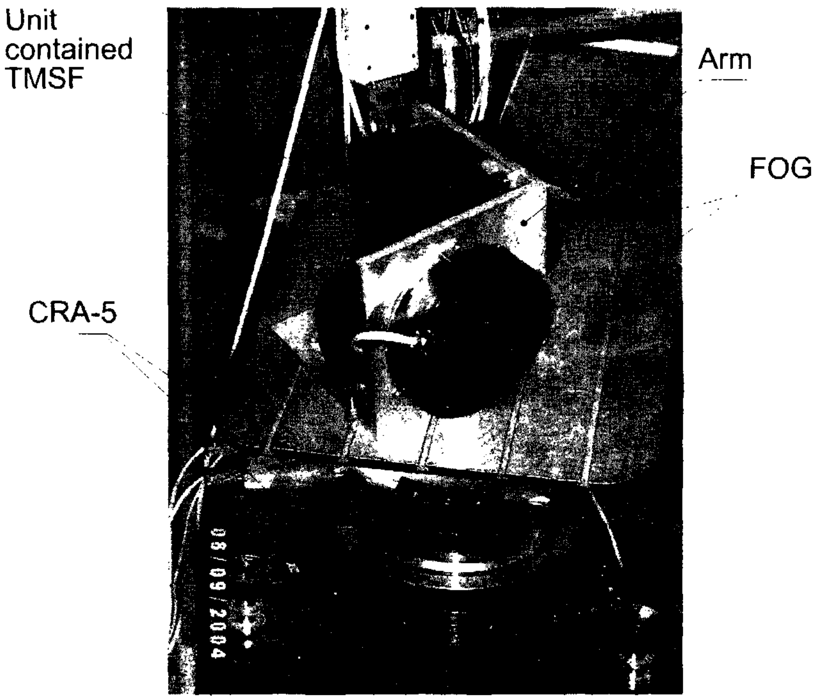

Fig. 4.

The accelerated alignment of system with the increasing factors of transfer of correction was made during 200 sec, then SGC was taken in a regular mode with adjustment to Schuler's frequency with account of the spherical model of the Earth. Experiments were done by setting of fixed angles of course of platform CRA-5 in azimuth on unlimited angles manually. In number of experiments the platform has been aligned in horizontal position, and in a number of experiments it was turned on the fixed angles of pitch and roll which values are from schedules.

After that SGC is turned on the course, and signals were observed on the screen of computer, and written to its memory then printing as figures.

In fig. 5 are shown the change of angle of course by indication of SGC and its errors for four fixed positions after flat turns on angles of course of platform CRA-5 with SIIM mounted on it. It is simply to see, that the course angle has changed from value approximately 0^0 up to value 90^0 (positive is angle Ψ which is measured from direction on the north in counter-clockwise). The error was up to $1,5^0$. In fig. 6 are shown the schedules of change of course angle, calculated with a signals of SGC, and its errors are shown. The schedules of fig. 5 and 6 present the transition of estimation of a course angle $\hat{\Psi}$ from the unsteady condition which is caused by noises of the TMSF, to steady at *t=200c*. During this moment of time SGC is switched to a mode corresponding to Schuler's conditions.

The error of an increment of a course angle reaches the value of *0,5 - 1,5 arc.deg*, and $\Delta\Psi = 45^0$ are observed in a transitive mode. We can explain these errors by instability of signals of micromechanical accelerometers. So, in time interval from 1200 up to 2400 sec the platform has constant orientation concerning the Earth. Signals of accelerometers by which angles $\hat{\theta}$ and $\hat{\gamma}$ are determined are unstable, that seen from fig. 6. They cause errors in determination of course angle. The analogical errors of course angle cause the instability of zero bias of FOGs.

For comparison in fig. 7 the errors of SGC taken with similar experimental algorithms are represented, but with taking into account nonsphericality of the Earth and with absence of errors of TMDAR and TMSF. Thus with 1200 on 20000 sec, with MO had rolling on all three corners Ψ, θ, γ relative to the Earth . We can see the fluctuations with the Schuler's frequency within the limits of angles of $\Delta\Psi \cong 3{,}2 arc.\sec$; $\Delta\theta \cong 10 arc.\sec$; $\Delta\gamma \cong 0{,}17 arc.\sec$. In fig. 7 the fluctuations of errors $\Delta\Psi$ caused by rolling of MO are shown in a magnifier mode. Mathematical modelling testifies that at presence of more precisely TMSF, than has been used in experiments, error of SGC can be reduced on several orders.

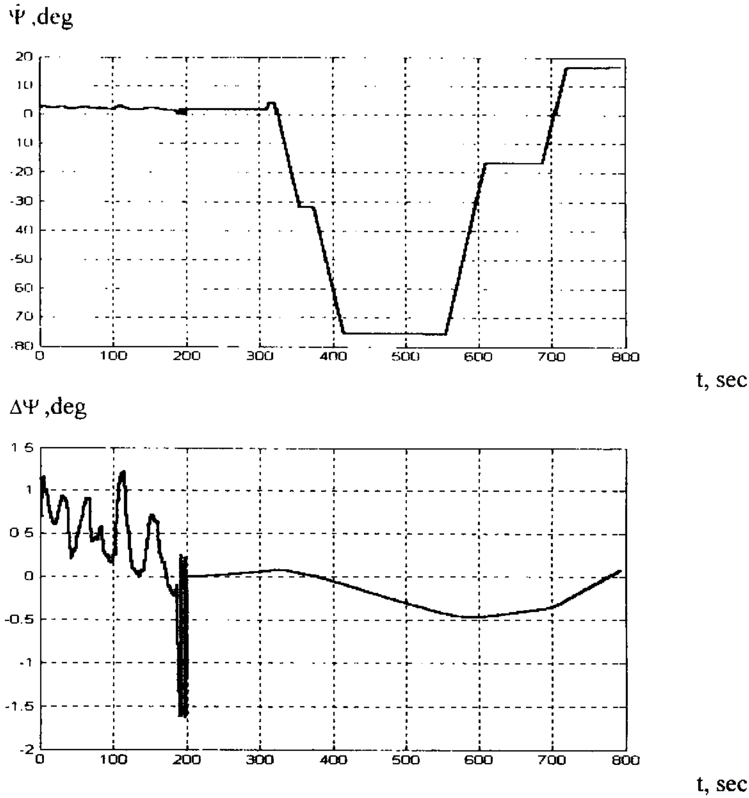

Ψ̂ ,deg
20
10
0
10
-20
-30
40
-50
60
70
-80
0
100
200
300
400
500
600
700
800
t, sec
ΔΨ ,deg
1.5
1
0.5
0
-0.5
-1
-1.5
-2
t, sec

Fig. 5.

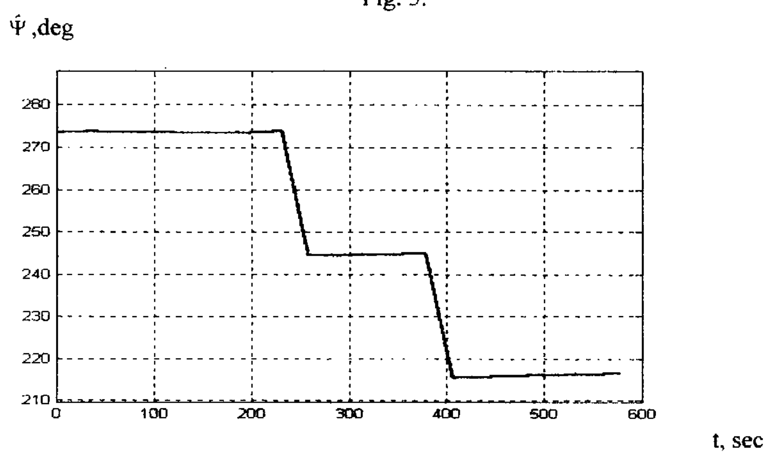

Ψ̂ ,deg
280
270
260
250
240
230
220
210
0
100
200
300
400
500
600
t, sec

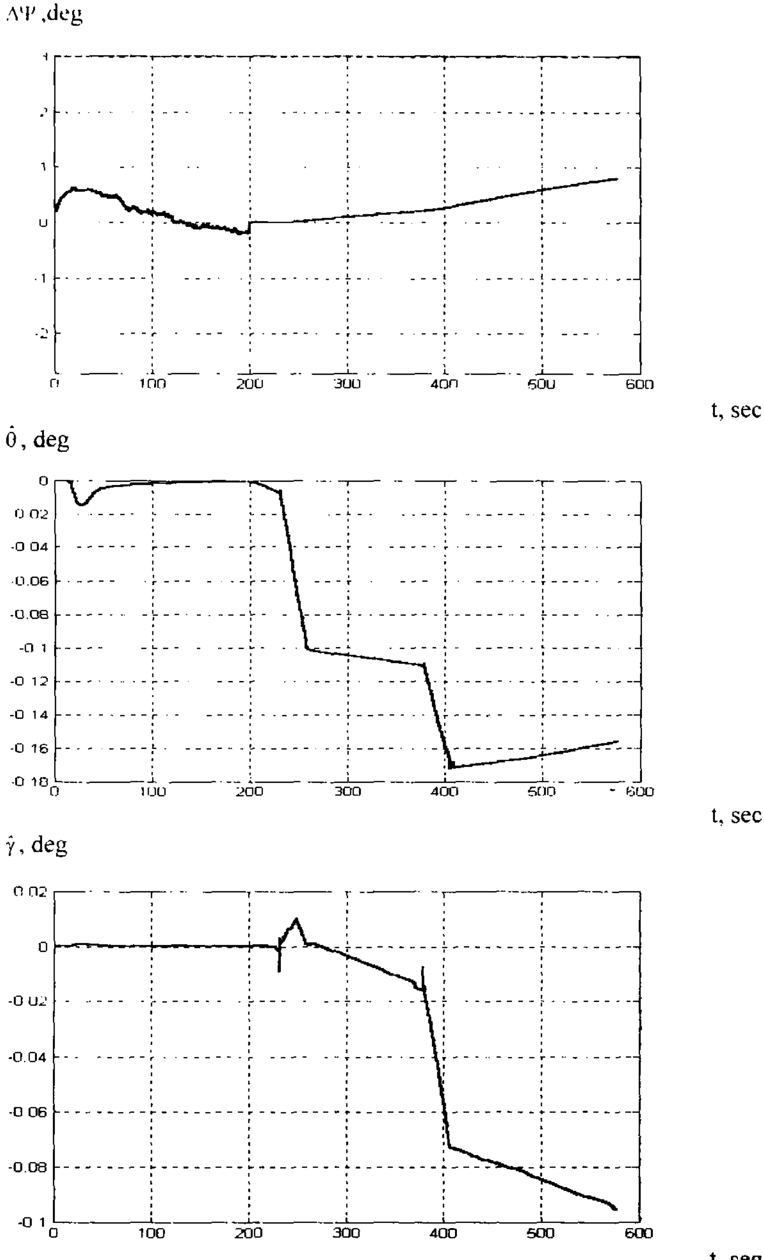
ΔΨ ,deg
0
1
-1
-2
0 100 200 300 400 500 600
t, sec
$\hat{\theta}$, deg
0
-0.06
-0.08
0 100 200 300 400 500 600
t, sec
$\hat{\gamma}$, deg
0
-0.04
-0.08
0 100 200 300 400 500 600
t, seg

Fig. 6.

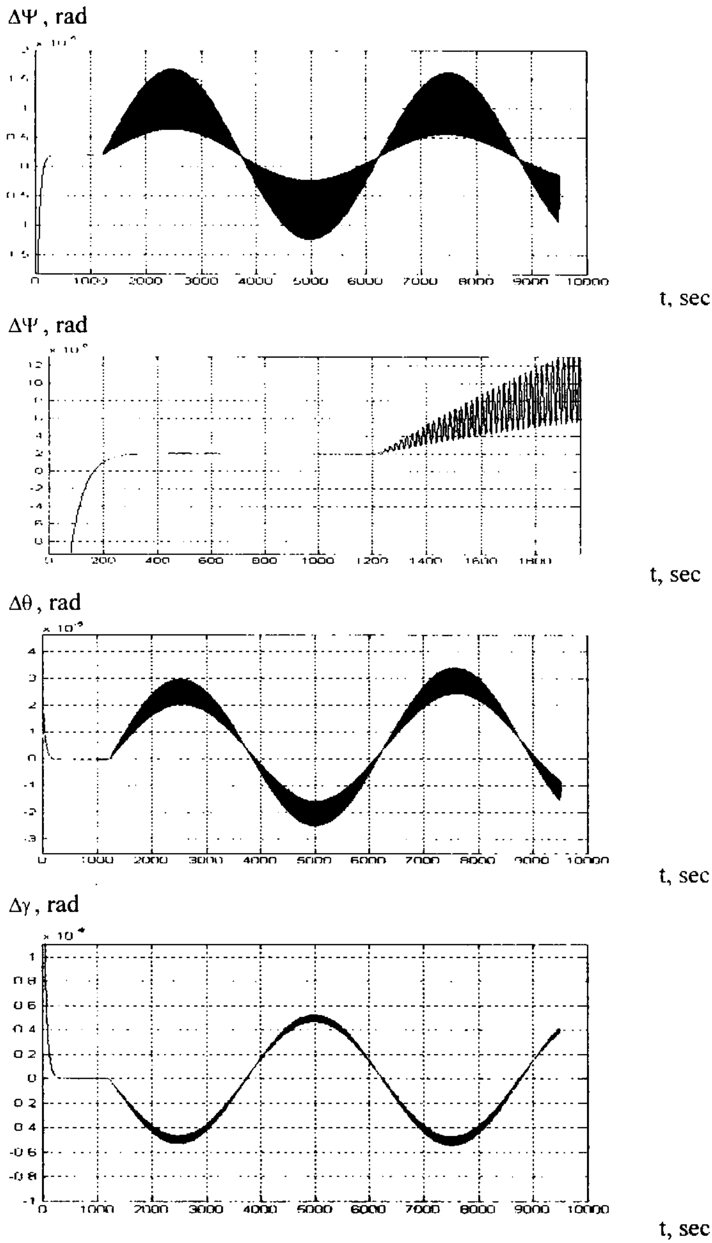

Fig.7.

Conclusions

1. Two versions of algorithms of SGC functioning are developed and tested in experiments under laboratory condition.
2. The equations and algorithms of mathematical modeling of functioning of SGC with account of ellipsoidal and also spherical model of the Earth are constructed.
3. The SGC mathematical model and corresponding data processing algorithms are developed with account of the spherical model as well as the ellipsoidal model of the Earth.

   Computer modeling of SGC operation has shown. In the case of ideal conditions and in presence of rolling the head angle error does not exceed *3,2 arc.sec.*

   With account of errors in FOG's and accelerometers $\Delta\omega_{ii} = 0{,}02\ {}^{\circ}/_{h}$; $\Delta W_{ii} = 10^{-4} g\ (i = \overline{1,3})$ the head angle error does not exceed *9 arc.min* for $2 \cdot 10^{4}$*sec* under the similar conditions.
4. The experimental study has shown that under conditions of instability of FOG zero bias less than 0,1 *arc.deg/hour* and zero bias instability of accelerometers less than *0,025* m/s^2 the head angle error in the stationary mode of SGC operation does not exceed *1 arc.deg.*

Reference

[1] T. Gaiffe, Y. Cottreau, N. Faussot, P. Simonpietri, H. Lefevre, H. Arditty. Marine fiber optic gyrocompass with integral motion sensor, Symposium Gyro Technology. 1999, Stutgart.

[2] SR 2100 Fiber Optic Gyrocompass & Attitude Reference System. KVH Industries. 2002.

[3] Wilfred Audi. Development of fiber optic gyroscopes and their application. SFIM Industries Deutschland GmbH Gotflieb-Daimler-Str. 60 D-71711. Murr., Germany, p.10.0-10.10

[4] F. Napolitano, T. Gaiffe, Y. Cottreau., T. Loret. First precision inertial system based on fiber optic gyros// Gyroscopy and navigation, 2002, №4(39), p. 101-114.

[5] Peshchonov V.G., Nesenjuk A.I., Staroseltsev L.P., Bagenov B.A., Buravlev A.S. Gyrohorizoncompass based on fiber optic gyros with rotable unit of sensors. Gyroscopy and navigation №1(36), 2002, p. 52-63.

[6] Dyott R.B., Allen D.E. A fiber optic gyroscope north finder// Proc. of 10th Optical fiber sensors cont. Glasgow Scotland, 11-13. Nov. 1994, h. 442

[7] Anuchin O.N., Emeliantsev G.I. Integrated system of orientation and navigation for sea mobile objects. Manual. –SPb.; CSRI «Electropribor», 1999, -357 p.

[8] Titterton D.H.. Weston. Strapdown Inertial Navigation Technology, 1997, IEE Radar, Sonar, Navigation and Avionics Series 5, London. - 455p.

[9] Plotnikov P.K The elements of theory of work of one version strapdown inertial systems of orientation // Gyroscopy and navigation, 1999, №4. p. 23-24.

[10] Tanaka T., Jagarashi Y. et al. Automatic north sensors using a fiber optic gyroscope// Applied Optics, 1994, Vol. 33 №1, p. 120-123.

[11] Plotnikov P.K., Nikishin V.B., Melnikov A.V., Skripkin A.A. Theory and Modelling of Functioning of Strapdown Autonomous and Corrected Gyroinclinometers. Symposium Gyro Technology, Stuttgart, Germany, 1995, p.p. 7.0-7.28

[12] Chebotarevsky J.V., Plotnikov P.K., Nikishin V.B. et al. Properties and Experimental Researches of Gyroinclinometers on the SINS Basis. Symposium Gyro Technology, Stuttgart, Germany, 2003, p.p. 21.0-21.13

[13] Ishlinsky Ju.A. Mechanics of gyroscopic systems. - M.: AS USSR Publishers. 1963 – 483p.

[14] Bromberg P.V. Theory of inertial systems of navigation. M.: Physmatgiz. 1979. – 295p.

[15] Plotnikov P.K., Nikishin V.B, Melnikov A.V. Determination of coordinates of a site of strapdown inclinometeer with account of nonspherisity of the Earth // Gyroscopy and navigation, №3(42), 2003, p. 45-51.